

Experimental Study on Tailings Deposition Distribution Pattern and Sedimentation Characteristics

Sen Tian,* Ying Zhao, Yuanheng Gong, and Guangjin Wang*



Cite This: *ACS Omega* 2024, 9, 19428–19439



Read Online

ACCESS |

Metrics & More

Article Recommendations

ABSTRACT: Tailings pond accidents frequently occur during an extended period, resulting in loss of life and property, wastage of resources, and environmental pollution. Relying on tailings pond engineering, this paper carried out sample particle fragmentation experiments and settling column experiments to explore the deposition distribution pattern of tailings in both horizontal and vertical directions as well as the impact of particle size distribution on the sedimentation stratification effect. The results show that the median particle size on the dry beach surface in the horizontal direction slowly decreased with the increase in the distance from the subdam. The particle size of tailings showed great fluctuations in the vertical direction, which gradually became finer with the increase in the depth overall. At the same time, saturated sedimentation experiments suggested the inconsistent variation rule with the field test, namely, coarse on the bottom and fine at the top, and the change in particle size greatly affected the tailing sedimentation stratification effect.

With the increase in fine particle content in tailings, the appearance time of the water–sand interface was shortened to within 30 min, but the sedimentation and consolidation completion times were delayed to about 1400 min. The settling column results indicate that the increase in fine particle content gradually weakened the sedimentation stratification effect, and the sedimentation pattern transformed from independent sedimentation to floc-type average sedimentation, which led to the enhanced water-retaining property of the settled layer. This may lead to an increase in the saturation line and a decrease in the length of the dry beach, seriously affecting the safe operation of the tailings pond. The research results provide some theoretical guidance and basic data for analyzing the consolidation efficiency of tailings and the stability of the tailings pond.



1. INTRODUCTION

With the development of the mining industry, safety problems caused by tailings have become one of the most serious problems in mining engineering. The research on tailings dam has thus attracted increasing attention.^{1,2} Tailings ponds are the places in which tailings pile and other industrial waste residues from metal and nonmetal mines reside after beneficiation.^{3,4} The sources of man-made and mud-rock flow have a high potential energy and potential risk of dam breaking.^{5–7} According to statistics, the number of dams has reached 12,000 in China, and tailings have grown by more than 600 million tons each year.⁸ Once an accident occurs, it may cause subsequent accidents such as landslides and debris flow, leading to the loss of life and property, wastage of resources, and environmental pollution.^{9–11} In the diverse damming technologies, the dam body of the tailings pond is mostly formed through the sedimentation and accumulation of the discharged tailings.¹² The sedimentation and consolidation rules of tailings will directly affect the dam body structure, including the dry beach length, dam body slope, and saturation line height, which is an important factor that affects the tailings pond stability and an important internal cause of the failure of the tailings pond.^{13–15} The settling column experiment can

also help us better understand the formation mechanism of cross-bedding and the lens during the sedimentation process of tailings. On the one hand, they may hinder the vertical seepage of tailings water and raise the saturation line of the dam body. On the other hand, their strength may decrease after being softened by immersion, making it easy to form potential sliding surfaces. Therefore, investigation of the sedimentation effect of tailings ore pulp and sedimentation and consolidation properties can not only provide basic data for the analysis of tailings pond stability but also optimize the damming pattern of tailings pond on this basis.

On the one hand, the engineering characteristics of tailings are not only determined by the physicomaterial properties but also related to the deposition characteristics.^{16,17} Due to the impacts of ore drawing, damming technique, tailings piling

Received: January 24, 2024

Revised: March 14, 2024

Accepted: March 14, 2024

Published: April 15, 2024





Figure 1. Engineering field of the tailings pond: (a) dry beach; (b) slope surface; (c) sampling points on dry beach surface; and (d) initial dam.

modes, tailings properties, and tailings dam type, there are variations of the tailings particle size at different deposition sites after hydraulic sorting,^{18–20} along with phenomena like cross-bedding, leading to the anisotropy of tailings dam body. The changes in particle size would result in variations in the dry beach and permeability of dam materials. That not only changes the length and slope of the dry beach but also affects the tailings deposition effect, finally affecting the stability of the tailings dam.^{21–23} Therefore, it is of great significance to analyze the characteristics of tailings particle size distribution for analyzing the tailings dam stability and guiding the optimization of the mine ore-drawing mode.

On the other hand, the sedimentation and consolidation properties of tailings are the key factors determining the overall consolidation deformation rules of the tailings dam.^{24,25} When the sedimentary properties of tailings are analyzed, settling columns are usually used for experiments. Some studies have proposed that computed tomography (CT) scanners and three-dimensional (3D) ultrasonic Doppler flow velocity profilers can be used to study the formation mechanism of sedimentary interlayers, suggesting that particle size is a key influencing factor in the formation of interlayers. Some scholars analyzed the influence of initial water content on the soil sedimentation property and discovered that the sedimentation stabilization time and the initial water content exhibited good power exponent relationship.^{26,27} Meanwhile, temperature and pH value also affect the pore water pressure and cohesion of tailings.^{28,29} However, tailing particle size distribution has a relatively more significant influence on sedimentation and consolidation. Some scholars carried out static sedimentation tests of ultrafine tailings to investigate the sedimentation time-history effect of tailings and compare the sedimentation and consolidation properties of sandy and viscous tailings in still water.^{30–32} With regard to numerical simulation, numerous studies simulated the grain flow based on the discrete element method to analyze the motion rules of different particles under water power.^{33–35} To sum up, the change in tailings particle size will affect the self-weight sedimentation and consolidation processes, which may lead to

changes in tailings pond parameters, such as dry beach surface and saturation line height.

Aiming at these problems, based on a practical upstream-method tailings dam, this study investigated the tailings deposition patterns on the dry beach surface and in the vertical direction of the tailings dam through field and laboratory experiments. Ulteriorly, saturated sedimentation experiments were carried out to explore the impact of particle size distribution on the sedimentation stratification effect. The research results would provide certain theoretical and practical guidance for the risk assessment of tailings dams and the optimization of the ore-drawing mode.

2. METHODOLOGY

2.1. Field and Laboratory Experiments. 2.1.1. Engineering and Geological Conditions. This tailings pond is located in Liangshan Prefecture, Sichuan, China, with an altitude of 430.80–1950 m. As the fault blocks midmountain terrain and platform midlow-mountain terrain, it is mainly characterized by structural erosion and secondary by erosion accumulation. The lithologies are clastic rock, carbonate rock, and volcanic sedimentary rock. The caprock strata are the Sinian Guanyinyan Formation, the Dengying Formation, and the Triassic Daqing Formation. The structure mainly shows the development of the northeastern fracture and nearly east–west compound anticlinal belt development. Because it is located at 26° north latitude, there is a clear distinction between dry and wet seasons under the influence of tropical monsoon. The average annual precipitation is 1124.9 mm, and the highest annual precipitation is 1661.6 mm.

The main deposits are iron and copper tailings. After expansion, the final stacking elevation is 2090 m and the total dam height is 147 m. The total storage capacity is 38.436 million m³, and the effective storage capacity is 33.893 million m³, which is second-class storage. The initial dam of the tailings pond consists of stone masonry. It has a crest elevation of 1941 m, a designed dam surface width of approximately 4.45 m, and a dam height of 32.7 m. As of May 2023, the usage elevation of the tailings pond has reached 2005 m at a dam

height of 63 m and the accumulated tailings are 3.2 million m³. The tailings pond is of valley type, with an altitude of 1945 m in the dam site area. As a terrain with alternating middle mountains and valleys, the slopes on both sides of the reservoir area are gentle, and the slope varies with the terrain by about 25–35°. Reservoir rock is mainly limestone, with stable mountains. The tailings are used for dam stacking, starting from the dam crest height of 1975 m. Through the upstream tailings dam construction method, the height of each subdam is 5 m, while the ratio of the subdam to the outer slope is 1:3.5. The coarse-grained tailings deposited in front of the reservoir are used to build subdams. The real engineering field of the tailing pond is shown in Figure 1.

2.1.2. Tailings Sampling and Screening. Tailings at the discharge outlet and different positions of the dry beach surface were selected as the samples for the experiment to investigate the horizontal deposition characteristics on the dry beach surface. Moreover, three sampling lines were set at appropriate locations on the dry beach surface, which were the approximate midline, and the sampling lines 75 m away from the midline at both sides (Figure 2). Additionally, three

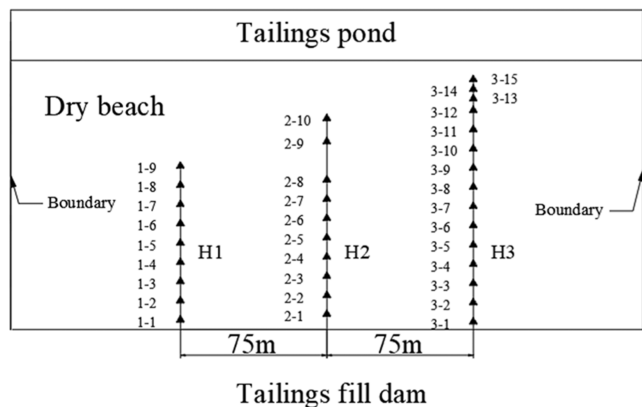


Figure 2. Positions of three sampling lines on the dry beach surface.

different vertical positions at the stacking dam were selected for drilling, and tailing samples at different depths were collected to analyze the vertical deposition characteristics of the tailings dam.

This study adopted the laboratory experiment to analyze the particle composition of the tailings sample. Therefore, the water screening method was selected when the particle size was over 0.074 mm (+0.074 mm),^{22,36} whereas the LS13320/VSM + laser particle analyzer was utilized for measurement when the particle size was less than 0.074 mm (−0.074 mm).

2.1.3. Statistical Analysis of Tailings Particle Composition. The original tailings were randomly selected and divided into five groups, numbered 1–5. The tailings content with particle sizes less than 0.074 mm (−0.074 mm) in the five groups was screened. The finest particle size of tailings is within the iron-

bearing tailings groups, the particle size of −0.074 mm ranges from 37.56 to 43.02%, with an average of 40.78%. Other results are indicated in Table 1.

2.2. Settling Column Experiments. The four groups of tailings samples (S_1 , S_2 , S_3 , and S_4) were collected from different positions on the dry beach surface of the tailings pond. The analytical test results of the particle size content are shown in Table 2.

Table 2. Particle Size Content of the Four Settling Groups

group no.	S_1	S_2	S_3	S_4
tailing content (−0.074 mm)/%	10.66	24.52	45.87	58.81

As shown in Figure 3, through full stirring, the samples were tested in flasks (diameter 5 cm × height 20 cm), and the process of the experiment with settling characteristics was recorded (at 0–1500 min) until the sedimentation stopped.

3. RESULTS AND DISCUSSION

3.1. Tailings Particle Gradation. Soil mass particle composition is one of the major factors affecting its physical–chemical properties, and the measurement indexes are coefficient of uniformity (C_u), coefficient of curvature (C_c), and median particle diameter (D_{50}), which are shown as follows³⁷

$$C_u = D_{60}/D_{10} \quad (1)$$

$$C_c = D_{30}^2/(D_{60} \times D_{10}) \quad (2)$$

where D_{10} is the mass of soil less than this size accounts for 10% of the total soil mass; D_{30} represents the mass of soil less than this size accounts for 30% of the total soil mass; and D_{60} denotes the mass of soil less than this size accounts for 60% of the total soil mass.

A greater C_u value indicates a higher degree of soil particle nonuniformity. Soil with a C_u value of greater than 5 is referred to as nonuniform soil; otherwise, it is called uniform soil. C_c reflects whether the slope of a curve is continuous.

The particle size composition is usually expressed as the average particle size³⁸

$$\bar{D} = \sum (R_i \times D_i) / \sum R_i \quad (3)$$

where D_i is the median of a particle size group and R_i indicates the percentage of the particle size group.

In Table 3, there is little difference in particle size between the tailings after rock elimination and the mixed tailings, while the iron-bearing tailings are obviously coarser than the former two. However, the particle size composition of the original tailings is normal overall.

3.2. Tailings Deposition Distribution Pattern.
3.2.1. Tailings Deposition Characteristics on Dry Beach Surface. When the tailings pulp is being discharged into the interior pond, the interactions between particles as well as

Table 1. Average Content of Original Tailings with a Particle Size Less Than 0.074 mm (−0.074 mm)

tailings type	tailing content (−0.074 mm)/%					average percentage/%	tailings type
	no. 1	no. 2	no. 3	no. 4	no. 5		
iron-bearing tailings	37.66	43.02	42.98	37.56	42.66	40.78	sandy silt
mixed tailings	52.25	46.85	53.92	49.86	53.31	51.24	fine sand
rock-eliminating tailings	51.88	47.97	52.02	46.89	52.44	50.24	sandy silt

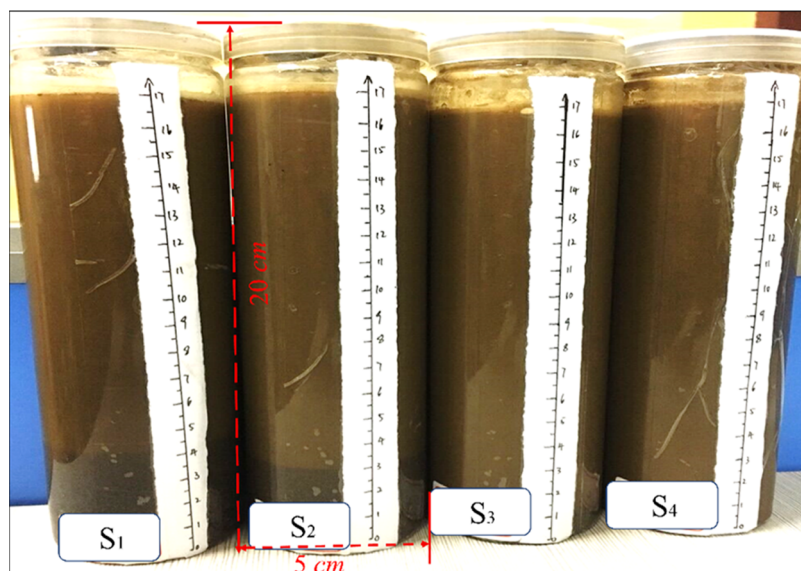


Figure 3. Settling column experiments.

Table 3. Statistical Characteristic Values of the Particle Size Composition of Original Tailings

sample	D_{10} (mm)	D_{30} (mm)	D_{60} (mm)	D_{50} (mm)	\bar{D} (mm)	C_u	C_c
iron-bearing tailings	0.0058	0.0411	0.1491	0.1104	0.0792	25.70	1.96
mixed tailings	0.0037	0.0196	0.0849	0.7081	0.0491	22.94	1.22
rock-eliminating tailings	0.0039	0.0233	0.0983	0.0756	0.0502	25.21	1.42

between particles and flow have resulted in extremely complicated motion of tailings particles on the dry beach surface.^{37,39} In order to understand the particle size distribution of tailings, the samples were collected at the tailings discharge outlet, in front of the dam, and at the pond tail, respectively, for the screening experiment.

In Figure 4, compared with the tailings particle size at the discharge outlet, the tailings particle size on the dry beach

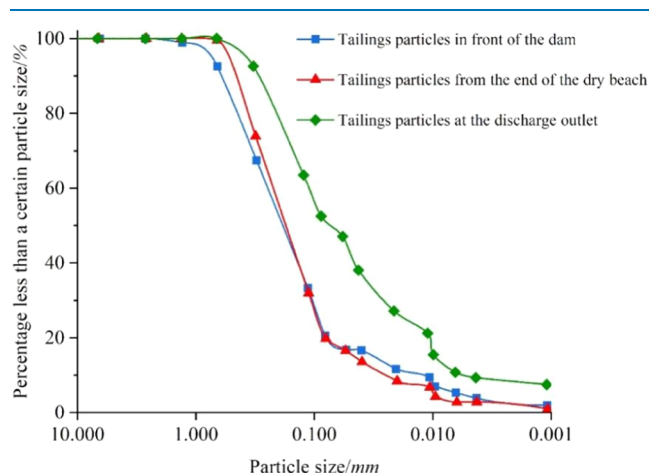


Figure 4. Gradation curves of tailings at different locations on the dry beach surface.

surface was significantly changed but was similar to the particle size changes in front of the dam and at the pond tail. It was suggested that, after discharging, the tailings were screened by water flow, the coarse particles deposited first, while the fine particles deposited later, so the tailings particles showed the

deposition characteristics of coarse anteriorly and fine posteriorly.

Figure 5 displays the tailings deposition distribution characteristics at three different locations on the dry beach

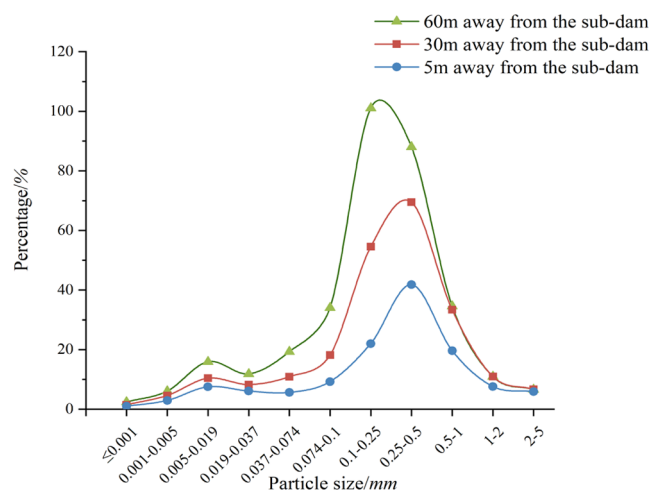


Figure 5. Particle content at different locations on the dry beach surface.

surface (5, 30, and 60 m away from the subdams on the dry beach surface). It is observed from the figure that the tailings show the rule of coarse anteriorly and fine posteriorly on the dry beach surface on the whole. First, at the location 5 m from the subdams, the tailings particle size mainly focused on 0.25–0.5 mm, while that at the 30 m location mainly focused on 0.1–0.25 mm, and that at the 60 m location focused on 0.1–0.25 mm. The reason was assumed that, after the tailings pulp was discharged, the coarse particles first deposited due to the

action of the self-supporting effect, and the small suspended particles flew to and deposited at the pond tail by the water flow. In addition, the tailings particle size did not greatly change at different locations, which concentrated in the range of 0.04–0.70 mm. This was mainly because of the uniform ore-drawing mode in front of the dam; in this way, the previously deposited tailings particles were rolled to the pond tail under the repeated current scour, so the overall particle size did not change greatly. Moreover, there was also a sudden change in particle size in the sample; when the particle size changed to the critical value, the content of tailings particles greater than the critical particle size significantly increased.

To more comprehensively characterize the variation law of tailings on the dry beach surface, three sampling lines (H_1 , H_2 , and H_3) were set at appropriate locations on the dry beach surface, which were the approximate midline, and the sampling lines 80 m away from the midline at both sides. Through the analysis of the samples taken, the particles on the dry beach surface are mainly constituted by the fine sand and sandy silt.

Figure 6 represents the average particle size of samples from different locations (equidistant sampling points) on the three

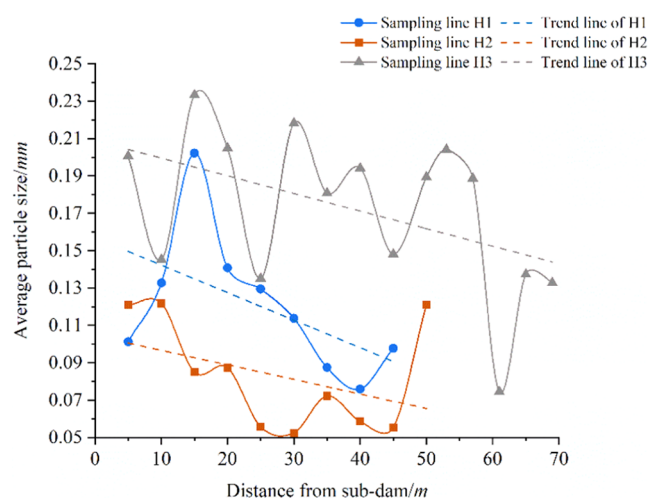


Figure 6. Average particle size of tailings on the dry beach surface.

sampling lines, which are numbered from close to far from the discharge outlet. The curves represent respectively the trend of average tailings particle size at different locations from the same sampling line to the subdam (discharge outlet nearby). It can be seen from Figure 6 that the average particle size becomes smaller with the increase of the distance from the subdam, which indicates that the finer particles are deposited in the tailings tail.

Figure 7 shows the curves of particle gradation (C_u and C_c) of tailings from the sampling points. It is stipulated in engineering that the soil with nonuniform particle composition ($C_u > 5$) and noncontinuous particle composition curve ($C_c = 1-3$) is rated as a well-graded soil. An analysis shows that the soil particle gradation of discharged tailings particles is changed from normal to abnormal, which is a great difference from those of the original tailings (in Table 2). The reasons are that the discharged tailings on the dry beach surface are affected by multiple factors, such as tailings pulp density, pond shape, discharge amount of the tailings, ore-drawing time, and damming method.

Furthermore, the contents of the -0.074 mm tailings particles were measured at three sampling lines on the dry beach surface. In Figure 8, the content of -0.074 mm tailings on the dry beach surface gradually increased with the increase in distance from the discharge point. In other words, after hydraulic classification, the tailings particles showed a deposition rule from coarse to fine between the discharge outlet and the interior pond. In the meantime, particle size coarsening was also observed at the local location, which was mainly related to flow separation. In the process of tailings pulp migrating to the deposition beach, the particle size and mass of coarse particles increased, which thus first deposited from the tailings pulp.

It was observed from Figure 8 that the tailings deposition rules on the dry beach surface were inconsistent. This might be because the multipipe subdivided flow dispersed ore drawing in front of the dam was adopted in that tailings pond; due to the paste impact, after the tailings pulp was discharged from the discharge pipe, it formed the impact energy dissipation pit around the discharge outlet. As a result, the tailings pulp flew around the energy dissipation pit and formed the fan-shaped

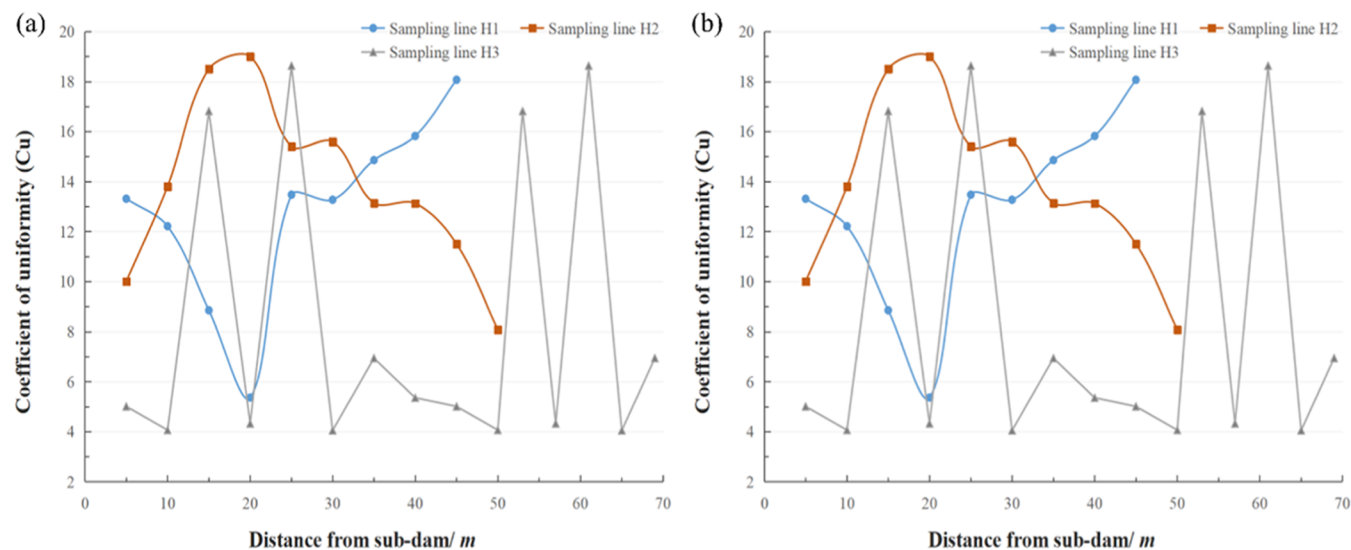


Figure 7. Particle gradation curves of tailings on the dry beach surface: (a) coefficient of uniformity (C_u) and (b) coefficient of curvature (C_c).

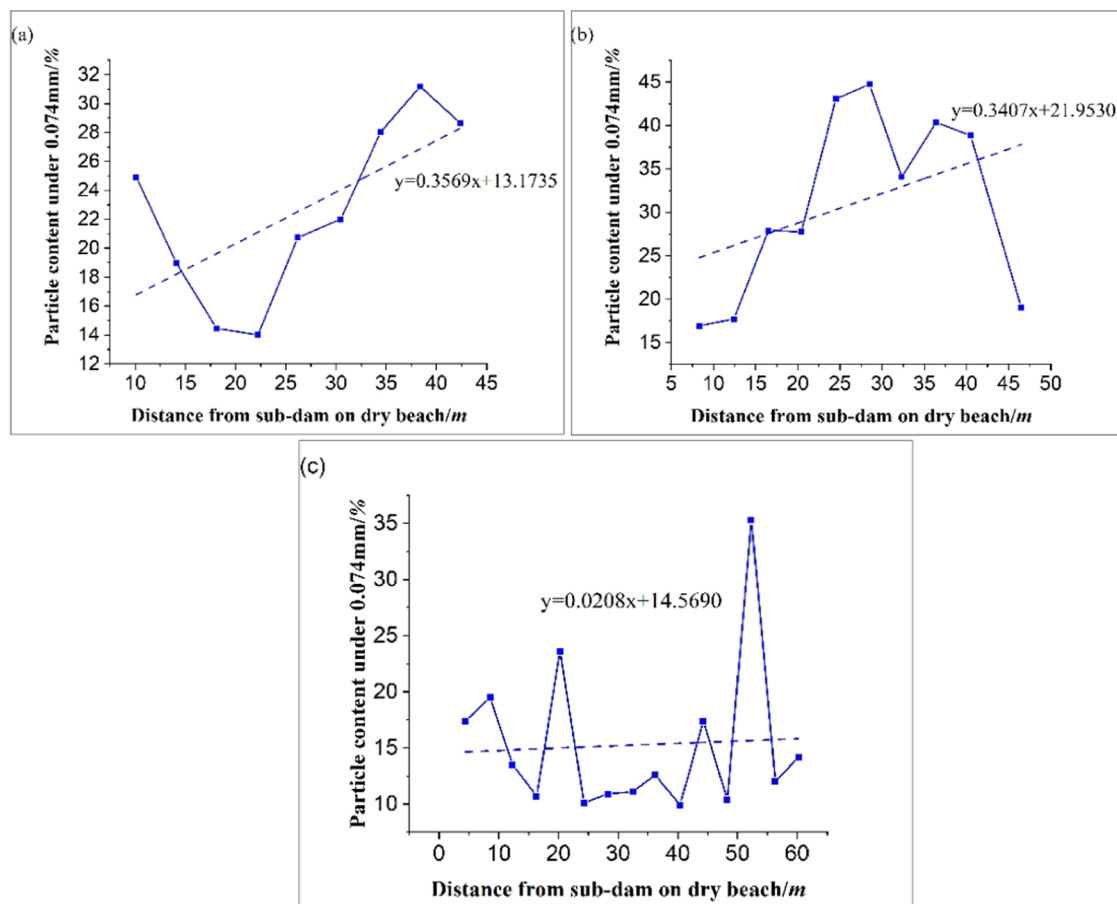


Figure 8. Particle content (−0.074 mm) of tailings on the sampling lines: (a) H₁, (b) H₂, and (c) H₃.

alluvial flat centered at the energy dissipation pit. The bed load tailings were deposited in the fan-shaped section, while the suspended load fine tailings were carried by the pulp to the pond tail, leading to the extremely apparent pond tail refining.

Figure 9 displays the relation curve of the median particle size (D_{50}) of tailings on three sampling lines with the distance from the subdam. As suggested by the fitted line, the D_{50} values at different positions on three measuring lines exhibited a gradually decreasing trend with the increase in distance from

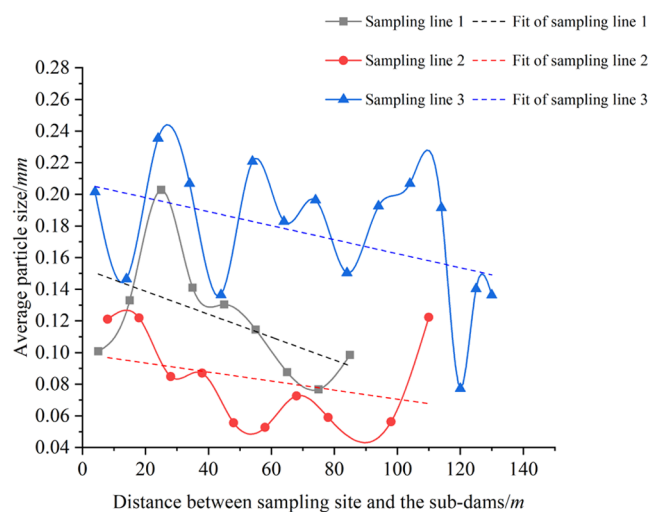


Figure 9. D_{50} of tailings on the sampling lines.

the subdam. This is because the repeated current scours during ore drawing lead to relatively even particle sedimentation on the dry beach surface.

3.2.2. Vertical Deposition of Tailings along the Fill Dam Body. The vertical deposition characteristics of the tailings dam are of great practical significance to analyzing the tailings dam generalized partitioning and dam body stability. In Figure 10, the average particle size gradually decreased with the increase in sampling depths. Through the comparative analysis of the sampling results at different locations (vertical lines V₁, V₂, and V₃) of the dam body, the changing trend of sandy silt is generally presented, and the particle size is mostly greater than 0.20 mm. When the sampling depth exceeds about 15 m, the particle size of the tailings decreases quickly. This was because due to alternated damming mode and the repeated current scour during the ore-drawing process, the coarse particles in front of the dam were carried by the water flow to the pond tail, while the small particles deposited at a more rapid rate vertically on the dam body.

In Figure 11, macroscopically, particle cross-bedding occurred at a local location. This was because the cross-bedding and lens were formed at the bending, concave, and convex areas of the gully after each round of ore drawing. However, phenomena like cross-bedding only took place within the vertical depth of 10–30 m from the dam body. This depth range mainly deposited the coarse particles at the previous subdams in front of the dam, leading to the significant difference in changes of coarse and fine particles. However, no similar phenomenon was observed within 10 m.

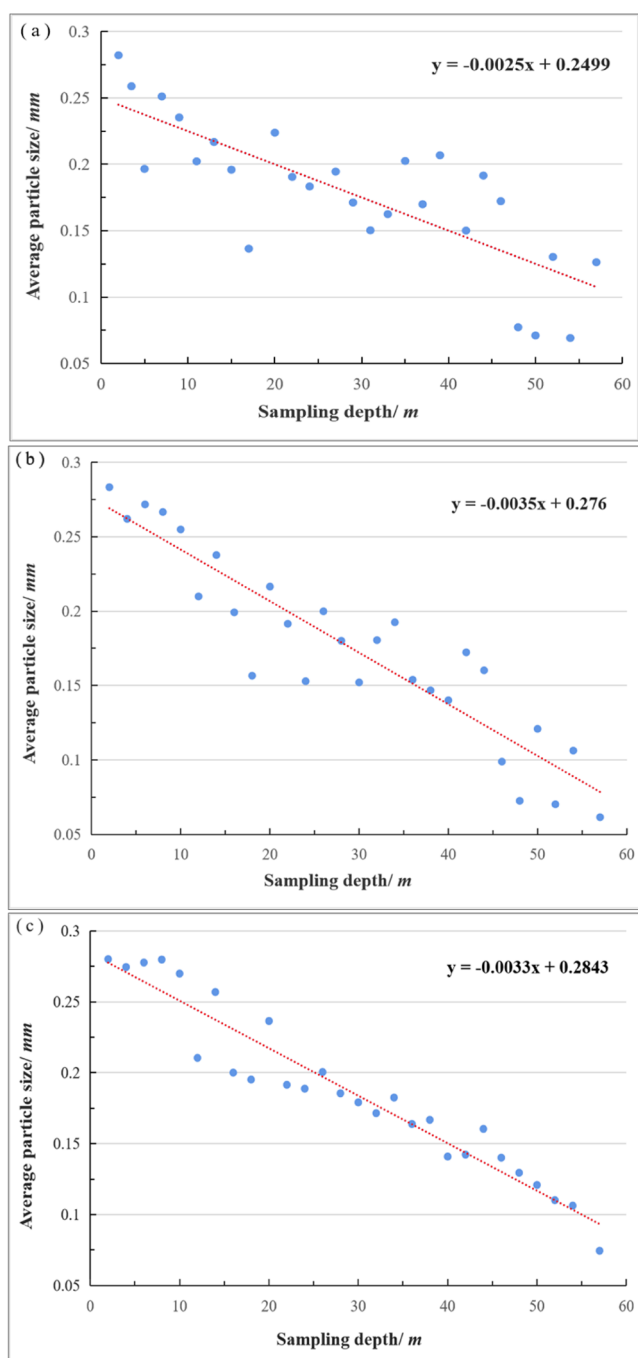


Figure 10. Average particle size of tailings at different locations (a) V_1 , (b) V_2 , and (c) V_3 .

3.3. Tailings Particle Sedimentation Properties.

3.3.1. Time Response Characteristics of Sedimentation. The stratification phenomenon during the tailing sedimentation process is related to the particle size distribution. As shown in Figure 12, groups S_1 and S_2 with a higher content of coarse particles immediately settled to the very bottom within 5 min after the initiation of the experiment and displayed the initial stratification phenomenon. In addition, they completed the sedimentation and consolidation within 600 min and exhibited the obvious sedimentation stratification phenomenon, but the obvious water–sand interface occurred within 30–100 min. By contrast, the S_3 and S_4 tailings pulps with a higher content of fine particles became clear within 30 min and

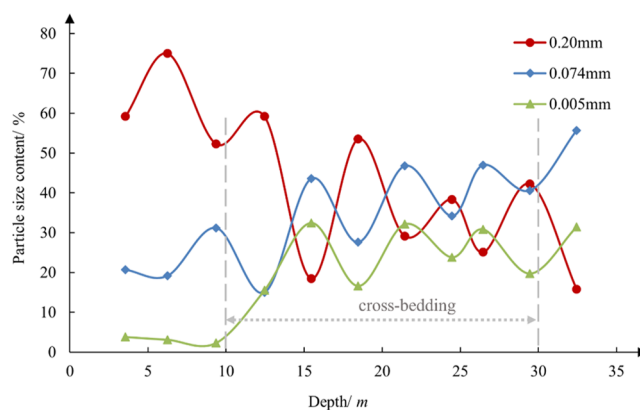


Figure 11. Variation of tailing particle sizes at different sampling vertical depths.

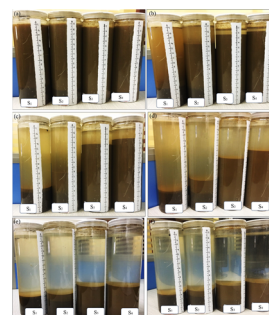


Figure 12. Settling column experiments process of tailings sample groups: (a) 5 min, (b) 30 min, (c) 100 min, (d) 200 min, (e) 600 min, and (f) 1500 min.

displayed a clear water–sand interface, but sedimentation and consolidation were completed at about 1500 min and did not show the obvious stratification phenomenon. Consequently, the greater fine particle content in tailings leads to the earlier occurrence time of the water–sand interface in the tailings pulp, and the final sedimentation time increases.

In the meantime, with the increase in fine particle content in tailings, the tailings changed from the single-particle sedimentation pattern to the floc-like sedimentation pattern, indicating that the finer particles make it easier for floc-type sedimentation and consolidation. This pattern can increase the water-retaining performance of tailings while decreasing the overall consolidation strength and may decrease the tailings pond stability.^{40,41}

During the tailings sedimentation test process, the rule of coarse on the bottom and fine at the top was observed, which was even significant in groups S_1 and S_2 with a higher coarse particle content. Nonetheless, with the advance of tailings sedimentation and consolidation, the fine particles gradually entered the pores between coarse particles under the action of overburden pressure; as a result, the coarsening effect on the bottom of tailings in groups S_1 and S_2 became weaker, leading to the phenomenon of coarse and fine particle interlayer and cross-stratification (Figure 13).

3.3.2. Sedimentation Stratification Characteristics. The sedimentation and consolidation of tailings are dynamic variation processes. Microscopically, the structure of the settled layer will change with time. Figure 14 shows the time–history curve of the tailings water–sand interface. The sedimentation of tailings pulp can be classified as natural

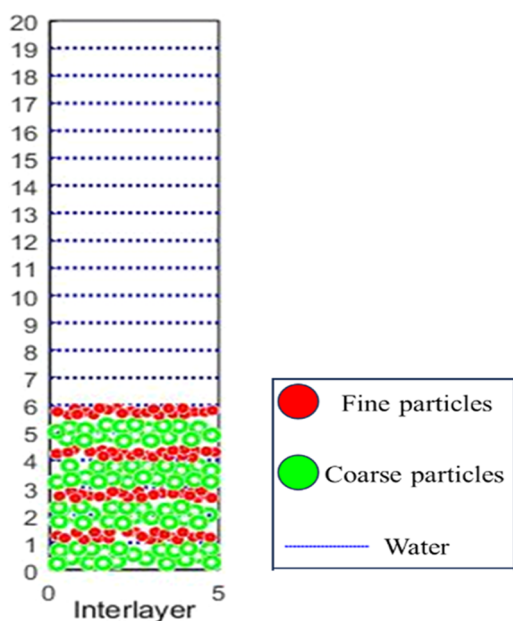


Figure 13. Diagram of tailings particle interlayer and cross-stratification.

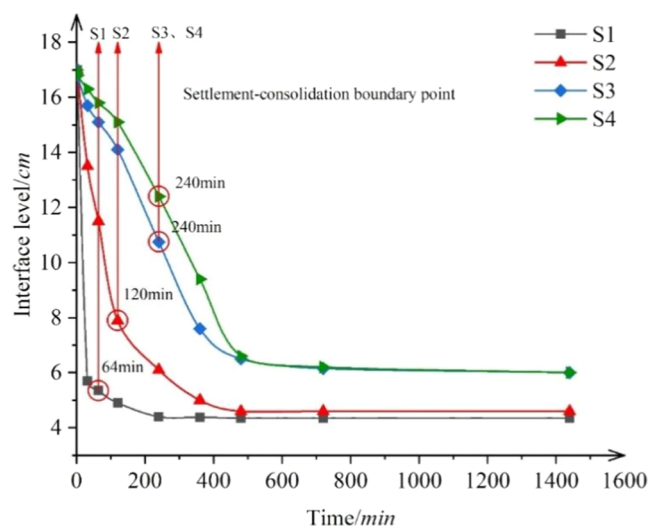


Figure 14. Time-course curve of tailings' water-sand interface.

sedimentation and self-weight consolidation stages. Of them, the sedimentation stage is a stage with rapid particle settlement and accumulation, which is characterized by a more rapid declining rate of water-sand boundary. In this stage, groups S_3 and S_4 showed the obvious water-sand interface within 32 min, while groups S_1 and S_2 exhibited the water-sand interface within 120 min. This could be because the group with a higher content of fine particles is more susceptible to cohesion between tailings particles and the formation of bulk flocculation phenomenon, thus settling to the bottom rapidly.

Meanwhile, the difference in particle size induced a substantial difference in the position of the water-sand interface among different groups. The sedimentation heights in groups S_1 and S_2 were 5.35 and 10.50 cm, respectively, whereas those in groups S_3 and S_4 were 15.35 and 15.55 cm, respectively, indicating that the sediment volume increased with the increase in fine particle content in the tailings pulp. This phenomenon demonstrates that the sediment density

decreases with the increase in fine particle content in tailings; at this moment, the sediment contains a lot of pores with soft texture, large volume, and low corresponding intensity.

Figure 15 shows the sedimentation process of tailings with different particle size distributions. As shown in the figure, after consolidation for a certain period, the height of the water-sand interface gradually decreased, and the consolidation volumes in groups S_3 and S_4 remained apparently greater than those in groups S_1 and S_2 . Thus, the dam body formed by tailings with a high content of fine particles in the early stage after discharge was relatively loose with low intensity.

In addition, particle size distribution significantly affects the occurrence time of the cutoff point between sedimentation and consolidation. The cutoff points in groups S_1 and S_2 occurred at 64 and 120 min, separately, while the sedimentation stage ended at about 240 min in groups S_3 and S_4 . From the cutoff point of sedimentation and consolidation to the end of consolidation stage, the settled layer heights in groups S_1 and S_2 with a large content of coarse particles showed little variation with time, and the differences in height were 0.37 and 0.12 cm, respectively (S_1 : 3.52 cm \rightarrow 3.15 cm, S_2 : 4.80 cm \rightarrow 4.68 cm), while there were large height differences in groups S_3 and S_4 (S_3 : 7.05 cm \rightarrow 5.45 cm, S_4 : 6.69 cm \rightarrow 5.45 cm), the differences in height were 1.60 and 1.24 cm, respectively. The tailing pulps in groups S_3 and S_4 exhibited a slow consolidation rate, a long duration, and a large amount of consolidation deformation. Therefore, for tailings with fine particle size, a longer time is needed for the entire sedimentation process in the pond after ore drawing, which is to the disadvantage of tailings pond stability.

Thereby, an obvious stratification phenomenon can be observed during the sedimentation process, but the phenomenon is weaker for tailings with a larger number of fine particles. In practical engineering, the weakening of the stratification phenomenon may lead to indistinct dam body stratification, a smaller dry beach surface, an elevated reservoir water level, and an elevated saturation line. In addition, with the increase in fine particle content, the sedimentation of tailings manifests as the floc-like overall sedimentation pattern, which is featured by a large water content inside, a longer time needed for sedimentation and consolidation than that of coarse particles, a larger volume, and a decreased water discharge capacity, regardless of the shorter solid-liquid separation time.

3.3.3. Tailings Consolidation Characteristics. As shown in Figure 16, during the sedimentation process, the settled layer on the bottom of the tailings exhibited fissures and interlayers. In Figure 16b, the tailings containing coarse particles were first deposited on the bottom. Due to the large pores between particles, the lower tailings experienced structural compression and a greater density under the action of overburden pressure and formed the consolidated fissures as shown in the figure. However, there was no obvious fissure in tailings containing fine particles due to the strong compressibility. In Figure 16a,c, because of the inconsistent shatter value between fine and coarse particles, the fine particles entered the pores between coarse particles on the bottom during the consolidation and water discharge process, which formed interlayers at different positions. As for tailings containing finer particles, the tailings were linked by a floc structure due to the small difference in tailing particle size; as a result, the water could hardly be discharged from the bottom, leading to the formation of the drainage channel.

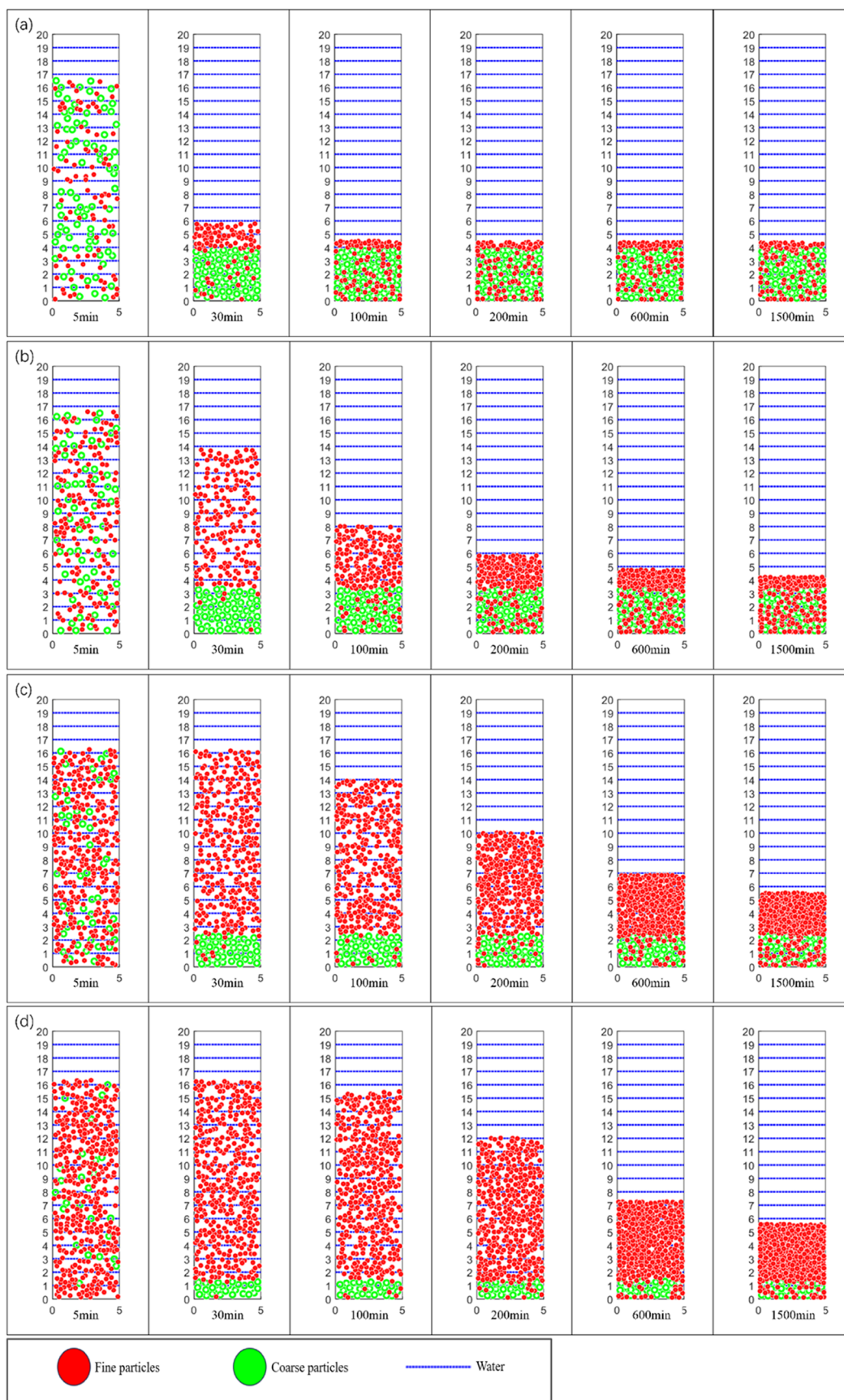


Figure 15. Process diagrams of water–sand interface variation of different tailings groups: (a) S_1 , (b) S_2 , (c) S_3 , and (d) S_4 .

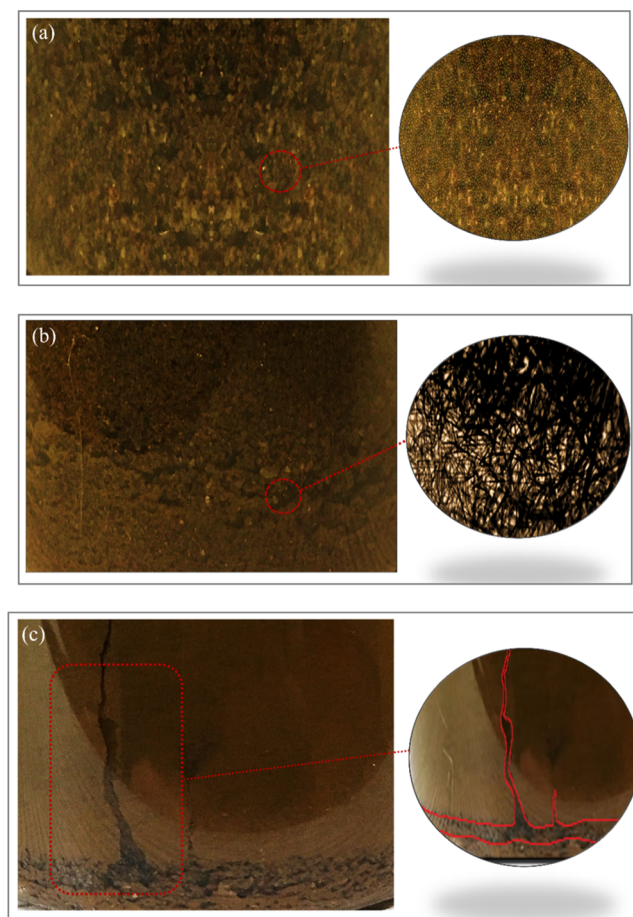


Figure 16. Partial view of tailings sedimentation consolidation characteristics: (a) interlayers, (b) cracks, and (c) main drain channel.

4. CONCLUSIONS

In this study, field and laboratory experiments are carried out to investigate tailings deposition distribution patterns and sedimentation stratification effect. The following conclusions are drawn.

The particle size of raw tailings in storage concentrated on 0.04–0.70 mm, while the C_u value of tailings particles on the dry beach surface decreased and the tailings size composition became worse after the discharge. On the dry beach surface, the farther distance between the subdam and the ore-drawing opening led to the smaller average particle size, and the deposition distribution exhibited the rule of coarse in front and fine in the distance. Effects like interlayer and cross-stratification induced by uneven particle size were observed locally, and the critical particle size phenomenon occurred at different positions. Moreover, the particle size of tailings showed great fluctuations in the vertical direction, which gradually became finer with the increase in the depth overall. When the sampling depth exceeds about 15 m, the particle size of the tailings decreases more quickly. The phenomena of cross-bedding and lenticel occurred at the bending, concave, and convex areas of the gully, and these phenomena mainly took place within the vertical depth of 10–30 m from the dam body.

According to the saturated sedimentation experiment, the tailing sedimentation in different groups displayed the rule of coarse on the bottom and fine at the top overall. The rule was more significant with the increase in particle size, accompanied

by a higher sedimentation rate and a higher probability of the stratification effect. With the increase in fine particle content, the tailings transformed from a single particle or floc sedimentation pattern to a flocculated network sedimentation pattern. In addition, as the sedimentation and consolidation process proceeded, the tailings coarsening effect on the bottom became weaker, while the coarse-fine interlayer occurred, leading to the anisotropy of the dam body, which affected its stability. For tailings with a larger amount of fine particles, the water–sand interlayer in the tailing pulp occurred earlier and the stratification phenomenon became weaker. At the same time, during the sedimentation process, fissures and interlayers were observed on the settled layer at the bottom of the tailings. Typically, fine-particle tailings are susceptible to consolidation fissures, while fine-particle tailings might form the drainage channel.

■ AUTHOR INFORMATION

Corresponding Authors

Sen Tian – State Key Laboratory of Coal Mine Disaster Dynamics and Control, School of Resources and Safety Engineering, Chongqing University, Chongqing 400044, China; School of Civil Engineering, The University of Queensland, Brisbane, QLD 4072, Australia; orcid.org/0000-0003-4725-959X; Email: sentian@cqu.edu.cn

Guangjin Wang – Yunnan Key Laboratory of Sino-German Blue Mining and Utilization of Special Underground Space, Faculty of Land Resources Engineering, Kunming University of Science and Technology, Kunming 650093, China; Email: wanguangjin2005@163.com

Authors

Ying Zhao – State Key Laboratory of Coal Mine Disaster Dynamics and Control, School of Resources and Safety Engineering, Chongqing University, Chongqing 400044, China

Yuanheng Gong – State Key Laboratory of Coal Mine Disaster Dynamics and Control, School of Resources and Safety Engineering, Chongqing University, Chongqing 400044, China

Complete contact information is available at: <https://pubs.acs.org/10.1021/acsomega.4c00138>

Author Contributions

S.T. was responsible for conceptualization, methodology, investigation, data curation, formal analysis, funding acquisition, supervision, project administration, writing the original draft, reviewing, and editing the manuscript. Y.Z. performed the methodology, data curation, and formal analysis and wrote the original draft. Y.G. was responsible for data curation and wrote the original draft. G.W. performed the methodology, data curation, formal analysis, validation, and project administration and wrote the original draft. All authors gave final approval for publication.

Notes

The authors declare no competing financial interest.

■ ACKNOWLEDGMENTS

This work was supported by the National Natural Science Foundation of China [Grant number 51904040], the General Program of Chongqing Natural Science Foundation Project [Grant number cstc2020jcyj-msxmX0747], the Fundamental

Research Funds for the Central Universities [Grant number 2020CDJ-LHZZ-003], the Venture and Innovation Support Program for Chongqing Overseas Returnees [Grant number cx2018071], and the Program for Changjiang Scholars and Innovative Research Team in University [Grant number IRT_17R112]. The authors would like to acknowledge the colleagues from the State Key Laboratory of Coal Mine Disaster Dynamics and Control for their perspectives and suggestions related to data collection and statistical analysis.

REFERENCES

- (1) Wang, T.; Zhou, Y.; Lv, Q.; Zhu, Y. L.; Jiang, C. A safety assessment of the new Xiangyun phosphogypsum tailings pond. *Miner. Eng.* **2011**, *24* (10), 1084–1090.
- (2) Kokangül, A.; Ulviye, P.; Cansu, D. A new approximation for risk assessment using the AHP and Fine Kinney methodologies. *Saf. Sci.* **2017**, *91*, 24–32.
- (3) Burritt, R. L.; Christ, K. L. Water risk in mining: analysis of the samarco dam failure. *J. Cleaner Prod.* **2018**, *178*, 196–205.
- (4) Kossoff, D.; Dubbin, W. E.; Alfredsson, M.; Edwards, S. J.; Macklin, M. G.; Hudson-Edwards, K. A. Mine tailings dams: Characteristics, failure, environmental impacts, and remediation. *Appl. Geochem.* **2014**, *51*, 229–245.
- (5) Zhang, W.; Long, J. H.; Zhang, X. R.; Shen, W. N.; Wei, Z. Y. Pollution and Ecological Risk Evaluation of Heavy Metals in the Soil and Sediment around the HTM Tailings Pond, Northeastern China. *Int. J. Environ. Res. Public Health* **2020**, *17*, No. 7072.
- (6) Wang, K.; Yang, P.; Hudson-Edwards, K. A.; Lyu, W.; Yang, C.; Jing, X. Integration of DSM and SPH to Model Tailings dam Failure Run-Out Slurry Routing Across 3D Real Terrain. *Water* **2018**, *10*, No. 1087.
- (7) Ismet, C. Guest editorial-Special issue on dynamic failures in underground mines. *Int. J. Min. Sci. Technol.* **2018**, *28*, iv–v.
- (8) Yin, G.; Li, G.; Wei, Z.; Wang, L.; Shui, G.; Jing, X. Stability analysis of a copper tailings dam via laboratory model tests: A Chinese case study. *Miner. Eng.* **2011**, *24*, 122–130.
- (9) Sun, E.; Zhang, X.; Li, Z. The internet of things (IOT) and cloud computing (CC) based tailings dam monitoring and pre-alarm system in mines. *Saf. Sci.* **2012**, *50* (4), 811–815.
- (10) Zheng, B.; Zhang, D.; Liu, W.; Yang, Y.; Yang, H. Use of Basalt Fiber-Reinforced Tailings for Improving the Stability of Tailings dam. *Materials* **2019**, *12*, No. 1306.
- (11) Nam, D. H.; Kim, M. I.; Kang, D. H.; Kim, B. S. Debris Flow Damage Assessment by Considering Debris Flow Direction and Direction Angle of Structure in South Korea. *Water* **2019**, *11*, No. 328.
- (12) Sun, G.; Cheng, S.; Jiang, W.; Zheng, H. A global procedure for stability analysis of slopes based on the Morgenstern-Price assumption and its applications. *Comput. Geotech.* **2016**, *80*, 97–106.
- (13) Santamarina, J. C.; Torres-Cruz, L. A.; Bachus, R. C. Why coal ash and tailings dam disasters occur. *Science* **2019**, *364*, 526–528.
- (14) Lumbroso, D.; McElroy, C.; Goff, C.; Collell, M. R.; Petkovsek, G.; Wetton, M. The potential to reduce the risks posed by tailings dams using satellite-based information. *Int. J. Disaster Risk Reduct.* **2019**, *38*, No. 101209.
- (15) Li, Z.-W.; Yang, X.; Li, T. Static and seismic stability assessment of 3D slopes with cracks. *Eng. Geol.* **2020**, *265*, No. 105450.
- (16) Wang, G. J.; Tian, S.; Hu, B.; Kong, X. Y.; Chen, J. An experimental study on tailings deposition characteristics and variation of tailings dam phreatic line. *Geomech. Eng.* **2020**, *23*, 85–92.
- (17) Zhu, L.; Zhou, T.; Ding, X.; Qin, X.; Zhang, J. Study on the Movement and Deposition of Particles in Supercritical Water Natural Circulation Based on Grey Correlation Theory. *Energies* **2019**, *12*, No. 2315.
- (18) Cao, G. S.; Wang, W. S.; Yin, G. Z.; Wei, Z. A. Experimental study of shear wave velocity in unsaturated tailings soil with variant grain size distribution. *Constr. Build. Mater.* **2019**, *228*, No. 116744.
- (19) Videla, A.; Faundez, D.; Meneses, J.; Gaete, L.; Vargas, Y. Enhancement of the sedimentation rate of copper tailings by application of acoustic fields. *Miner. Eng.* **2020**, *146*, No. 106096.
- (20) Kinnarinen, T.; Tuunila, R.; Hakkinen, A. Reduction of the width of particle size distribution to improve pressure filtration properties of slurries. *Miner. Eng.* **2017**, *102*, 68–74.
- (21) Adiguzel, D.; Bascetin, A. The investigation of effect of particle size distribution on flow behavior of paste tailings. *J. Environ. Manage.* **2019**, *243*, 393–401.
- (22) Tian, S.; He, Y.; Bai, R.; Chen, J.; Wang, G. Experimental study on consolidation and strength properties of tailings with different particle size distribution characteristics. *Nat. Hazards* **2022**, *114* (3), 3683–3699.
- (23) Ma, C.; Li, R.; Zhang, C.; Guo, X.; Li, X. A study on compressibility and permeability of tailings with different particle sizes under high pressure. *Bull. Eng. Geol. Environ.* **2023**, *82* (4), No. 106.
- (24) Bonin, M. D.; Cabral, A. R.; Nuth, M. Examination of the Effects of Solids Content on Thickened Gold Mine Tailings Sedimentation and Self-Weight Consolidation. *Geotech. Test. J.* **2019**, *42* (6), 1493–1517.
- (25) Lebitsa, G.; Heymann, G.; Rust, E. Excess pore pressure generation during slurry deposition of gold tailings. *Int. J. Min., Reclam. Environ.* **2021**, *35* (2), 95–114.
- (26) Dong, H. N.; Horpibulsuk, S.; Suddepong, A.; Hoy, M.; Chinkulkijniwat, A.; Arulrajah, A.; Chaiwan, A. Compressibility of ultra-soft soil in the Mae Moh Mine, Thailand. *Eng. Geol.* **2020**, *271*, No. 105594.
- (27) Lee, M.-S.; Oda, K. Self-Weight Consolidation Prediction Method Considering Properties of Segregating Sedimentation. *Geotech. Test. J.* **2019**, *42* (1), 194–220.
- (28) Abdunabi, A.; Beier, N. A.; Smith, L.; Smith, H. L.; Macdonald, G. Comprehensive Geotechnical and Geochemical Characterization of two Diamond Ore Tailings. *Environ. Geotech.* **2022**, 1–11.
- (29) Niu, F.; Zhang, H.; Zhang, J.; Yu, X. Temperature Variation Characteristics and Model Optimization of Flocculation Sedimentation of Overflow Ultra-Fine Iron Tailings. *Minerals* **2022**, *12* (5), 643.
- (30) Niu, F.; Zhang, H.; Zhang, J.; Yu, X.; Wang, W. Coagulation sedimentation performance and model optimization of ultra-fine tailings overflow from hydrocyclone. *Miner. Eng.* **2022**, *186*, No. 107737.
- (31) MacIver, M. R.; Hamza, H.; Pawlik, M. Effect of suspension conductivity and fines concentration on coarse particle settling in oil sands tailings. *Can. J. Chem. Eng.* **2021**, *99* (9), 2024–2034.
- (32) Cabrera, S. M.; Motta, B. J.; Komishke, B.; Kantzas, A. Study of the settling characteristics of tailings using nuclear magnetic resonance technique. *Int. J. Min., Reclam. Environ.* **2009**, *23* (1), 33–50.
- (33) Ming, L. Q.; Hong, Z.; Jie, W.; Yun, Z. Numerical Simulation on the Evolution of Tailings Pond Dam Failure Based on GDEM Method. *Front. Earth Sci.* **2022**, *10*, No. 901904.
- (34) Chen, S.; Jin, A.; Zhao, Y.; Wang, J. Equivalent numerical method and sensitivity analysis of microparameters for micropore compression stage of cemented tailings backfill. *Constr. Build. Mater.* **2023**, *369*, No. 130490.
- (35) Wang, D.; Ho-Minh, D.; Tan, D. S. Discrete element modelling of sediment falling in water. *Eur. Phys. J. E* **2016**, *39* (11), No. 112.
- (36) Lee, U. J.; Hyeong, K. S.; Cho, H. Y. Estimation of Settling Velocity and Floc Distribution through Simple Particles Sedimentation Experiments. *J. Mar. Sci. Eng.* **2020**, *8* (7), No. 500.
- (37) Wang, X. Z.; Shan, H. G.; Wu, Y.; Meng, Q. S.; Zhu, C. Q. Factors affecting particle breakage of calcareous soil retrieved from South China Sea. *Geomech. Eng.* **2020**, *22*, 173–185.
- (38) Shen, J. H.; Xu, D. S.; Liu, Z. W.; Wei, H. Z. Effect of particle characteristics stress on the mechanical properties of cement mortar with coral sand. *Constr. Build. Mater.* **2020**, *260*, No. 119836.
- (39) Ormann, L.; Zardari, M. A.; Mattsson, H.; Bjelkevik, A.; Knutsson, S. Numerical analysis of strengthening by rockfill embankments on an upstream tailings dam. *Can. Geotech. J.* **2013**, *50* (4), 391–399.

(40) Gan, D. Q.; Yang, X.; Zhang, Y. P. Permeability Prediction of Iron Tailings Including Degree of Compaction and Structure. *Complexity* **2019**, *2019*, No. 3591628.

(41) Rico, M.; Benito, G.; Diez-Herrero, A. Floods from tailings dam failures. *J. Hazard. Mater.* **2008**, *154*, 79–87.